J. Phys. I France **3** (1993) 107–134 JANUARY **1993**, PAGE 107

Classification
Physics Abstracts
63.20D

Scaling properties of vibrational spectra and eigenstates for tiling models of icosahedral quasicrystals

J. Los ([1]), T. Janssen ([1]) and F. Gähler ([2])

([1]) Institute for Theoretical Physics, University of Nijmegen, 6525 ED Nijmegen, The Netherlands
([2]) Département de Physique Théorique, Université de Genève, 24 quai Ernest Ansermet, CH-1211 Genève, Switzerland

(Received 11 August 1992, accepted in final form 1 October 1992)

Abstract. — A study of the lattice dynamics of 3-dimensional tilings modelling icosahedral quasicrystals is presented, both in commensurate approximations and cluster approximations. In the commensurate approximation this is done for three different types of tilings, namely: perfect, symmetrized and randomized approximants. It turns out that the density of states as a function of frequency is smoothed by randomization. A multifractal analysis of the spectrum shows that mainly at high frequencies the scaling behaviour of the spectrum is different from that for periodic structures. Also the eigenvectors are examined and it appears that only the states at the very upper end of the spectrum have a relatively small participation fraction, i.e. are more localized. The majority of the states scale as normal extended states, as is shown by a multifractal analysis of the eigenvectors for systematic approximants. Also, for most of the states localization is not enhanced by randomization. Throughout the paper the results are compared with those for a 1-dimensional quasicrystal, the Fibonacci chain.

1. Introduction.

The first calculations of the lattice dynamics of 3-dimensional models of icosahedral quasicrystals were published in reference [1]. Here we present a further study of the lattice dynamics of 3-dimensional icosahedral Penrose tilings (i-PT's), which are closely related to the structure of icosahedral quasicrystals, discovered by Shechtman et al. in 1984 [2].

The i-PT has no 3-dimensional lattice periodicity but is quasiperiodic. Therefore calculations of physical properties, such as phonons and electronic states, are much more difficult than in ordinary, periodic structures. In [1] we have presented numerical calculations of the phonon spectrum of symmetrized clusters and rational approximants in a simple dynamical model. In the present paper not only the spectrum but also the eigenvectors are considered. This will also be done for so-called randomized tilings, which are constructed from perfect quasiperiodic tilings or rational approximants by repeatedly flipping certain atomic positions. Differences

between the vibrational spectra of perfect and randomized tilings might give us a mean to distinguish between such structures experimentally. It is known that the randomized tilings, or random tilings, as they are usually called, are very well acceptable as models for real quasicrystals [3, 4].

The density of states $D(\omega)$ is defined such that $D(\omega)\mathrm{d}\omega$ is equal to the number of states between ω and $\omega + \mathrm{d}\omega$. For ordinary crystals with only a few atoms in the unit cell the density of states (DOS) is a smooth function of ω with only a few singularities (van Hove singularities). These singularities are due to points in the phonon branches for which $\mathbf{n} \cdot \nabla_k \omega_s(\mathbf{k}) = 0$ holds, where $\omega_s(\mathbf{k})$ is the s^{th} phonon branch as a function of the wave vector $\mathbf{k}$ and $\mathbf{n}$ is a unit vector orthogonal to the branch surface at $\mathbf{k}$. The i-PT is the limit of a sequence of approximants with more and more atoms inside the unit cell and thus, since the number of branches is 3 times the number of atoms in the unit cell, a large number of singularities might occur in the spectrum. These singularities will not be strong however, since the Brillouin zone is small for structures with large unit cells, and thus only in the fine structure an irregular behaviour of the DOS can be expected. Globally one expects that the DOS is smeared out. In the randomized tilings the local order is partially lost. It is likely that this loss of order is also visible in the DOS.

For several 1-dimensional quasiperiodic structures, including also the 1-dimensional quasicrystals, it has been shown that excitation spectra have a character different from that of periodic crystals. In the latter case the spectrum consists of a number of bands and is absolutely continuous. All states are extended Bloch-waves. It is known that for completely random 1-dimensional structures the spectrum is a pure point spectrum with correspondingly localized states, i.e. states with an exponential decay of the wave function outside a bounded region. This also holds for 2-dimensional random structures, but not for 3-dimensional random structures where part of the states may be normally extended. For the Fibonacci chain, which is a 1-dimensional quasicrystal, it was shown [5, 6] that the vibrational spectrum is neither absolutely continuous nor a point spectrum but so-called singularly continuous, with correspondingly critical states. Examples of such states are states showing an intermittent behaviour, i.e. they are essentially localized on several disconnected bounded regions.

As a comparison we have reconsidered the lattice dynamics of the Fibonacci chain. The character of the spectrum and the wave vectors have been studied using the same numerical approach as for the 3-dimensional tilings. The Fibonacci chain can be considered as a 1-dimensional quasiperiodic sequence of long and short intervals, which remains invariant under the following inflation rule: replace each long interval by a long and a short interval, replace each short interval by a long interval. In our study of the dynamics of this system we simple placed atoms with mass $m = 1$ on the vertices and connected neighbouring atoms by springs with spring constant $K = 1$ for a long interval and $K = 3$ for a short interval.

To determine the character of spectra of 1-dimensional systems Kohmoto [7] introduced a multi-fractal analysis, based on a thermodynamical formalism. In this paper we show how this method can be generalized for systems in arbitrary dimension, and results are presented for several periodic i-PT approximants. Since the multifractal analysis only gives information on the character of the spectrum of the i-PT if one is able to predict what happens in the limit to the infinite quasiperiodic system, the results for only a couple of smaller approximants may not be sufficient to draw any definitive conclusions. Nevertheless, a lot of useful information is obtained, also because we can compare with the corresponding results for the Fibonacci chain, for which the behaviour in the infinite limit is known analytically.

Kohmoto's multifractal analysis of the wavevectors (wavefunctions) does not need to be generalized to more than one dimension, since it works the same way in any dimension. The method is intended to give information about the scaling behaviour of the eigenvectors under

enlargement of the system.

Concerning the multifractal analysis, we will introduce some further extensions to it, which enables us to compare properly the multifractal properties of spectra and wavefunctions for different systems of (different) finite size. Our approach is especially useful for analyzing carefully the convergence of the results for systematic approximants of systems which can not be analyzed analytically, due to the lack of lattice translational symmetry.

The paper is organized as follows. In section 2 the structure of i-PT's and closely related tilings such as symmetrized tilings, rational approximants and randomized tilings are explained. Then the dynamical model is defined. In section 3 the DOS is presented for various tilings, and special attention is paid to the effect of randomization. It is also studied whether the DOS is sensitive to the kind of interaction that is used. In section 4 a generalization of the multifractal analysis of spectra for sytems in arbitrary dimension is given and applied to perfect, symmetrized and randomized i-PT approximants. In section 5 the participation fraction, which is a measure for the number of atoms participating in a certain eigenmode, is studied as function of frequency for clusters and various approximants. Furthermore a numerical approach to study the scaling behaviour of the eigenvectors, based on the multifractal analysis, is proposed and applied to systematic approximants. Both in sections 4 and 5 the results are compared with the corresponding results for the Fibonacci chain. Section 6 contains our conclusions.

2. Structure and dynamical model.

2.1 THE ICOSAHEDRAL PENROSE TILING. — The 3-dimensional icosahedral Penrose tiling (i-PT) (see e.g. [8]) is space filling with two kinds of 'tiles', a thick and a thin rhombohedron. The thick rhombohedron occurs ϕ times more often than the thin one, where $\phi = (\sqrt{5}+1)/2$ is the golden mean. The i-PT is quasiperiodic and can be obtained as the intersection of a 6-dimensional periodic structure with a 3-dimensional subspace V_E, called physical space or external space. The 6-dimensional lattice can be chosen to be hypercubic. In Cartesian coordinates a basis for it is given by:

$$\begin{array}{ll} a_1 = (1,\phi,0,1,\phi,0) & a_2 = (-1,\phi,0,1,-\phi,0) \\ a_3 = (0,1,\phi,-\phi,0,-1) & a_4 = (\phi,0,1,0,-1,\phi) \\ a_5 = (\phi,0,-1,0,-1,-\phi) & a_6 = (0,1,-\phi,-\phi,0,1) \end{array} \qquad (1)$$

The first three components of these vectors are in external space V_E, whereas the last three are in internal space V_I, which is perpendicular to V_E. These two spaces are separately left invariant by icosahedral symmetry. The projections of the six basisvectors and their negatives on either of the two spaces point to the vertices of an icosahedron.

The 6-dimensional periodic structure consists of an array of 3-dimensional polyhedra, which are called atomic surfaces. For the i-PT the atomic surface is a triacontahedron, which is obtained as the projection of the 6-dimensional hypercubic unit cell on V_I. On each lattice point of the 6-dimensional lattice such a triacontahedron is placed parallel to V_I, such that the lattice points are the centres of the triacontahedra. The vertices of the tiling, which will be used as atomic positions, are obtained as the intersections of external space V_E with the atomic surfaces.

Although the symmetry requirements fix the orientation of external space relative to the lattice one still has the freedom to shift V_E along an internal direction, parallel to V_I. In order to obtain the vertices of a true i-PT, made of rhombohedral tiles, we must take care that external space never touches any 0-, 1- or 2-dimensional boundary of an atomic surface. In the present case this implies in particular that external space must not pass through any lattice

point nor through any 6d body centre of the cubic lattice, which is the reason why there are no i-PT's with exact icosahedral symmetry.

Positions of external space for which V_E intersects the boundary of an atomic surface are called singular. To ensure that the tilings corresponding to a singular positions of V_E are still tilings with the same two rhombohedra, an infinitesimal shift of V_E to a non-singular position has to be applied, which makes sure that only half of the boundaries are included in the atomic surfaces. Singular positions can be resolved in two or more inequivalent ways, so that there are several i-PT's corresponding to such positions. In a certain sense i-PT's corresponding to a singular position of V_E can be understood as the limit of a sequence of i-PT's corresponding to non-singular positions.

If we insist on a structure with exact icosahedral symmetry we may let V_E pass through a lattice point (i.e. the centre of an atomic surface) and make an ad hoc assignment on which parts of the boundaries of the atomic surfaces should be included. We only have to make sure that this assignment respects icosahedral symmetry. The price we have to pay then is that the resulting structure is not the set of vertices of a true i-PT made of rhombohedra, but a more general quasiperiodic structure (see Sect. 2.3).

Another characteristic of the i-PT concerns its scaling property. This means that a certain subset of the vertices of the i-PT form the set of vertices of an new i-PT consisting of rhombohedra that are now ϕ^3 times larger then the original ones.

2.2 Related tilings.

2.2.1 *Commensurate approximations.* — One can obtain 3-dimensional lattice periodic approximants of the i-PT by slightly deforming the 6-dimensional structure. This can be done in different ways, and a general analysis has been made by Janssen [10]. Here we give a brief summary of the results. To obtain a lattice periodic structure one replaces the ϕ's in the internal components of the six basis vectors by rational numbers. A sequence of rational numbers which give increasingly accurate approximations of the irrational value ϕ is given by $\phi_n = F_n/F_{n-1}$, where F_n are the Fibonacci numbers, i.e. $F_{-1} = 0$, $F_0 = 1$, $F_{n+1} = F_n + F_{n-1}$. Notice that the atomic surface, which now is the projection of the deformed 6-dimensional unit cell on the internal space, is also deformed by this substitution. If the same rational value is used in each of the three internal components the structure in physical space will have a cubic lattice of translational symmetries. These approximants are denoted as the 1/1-, 2/1-, 3/2-,.. approximants. In the cases where $F_n + F_{n-1}$ = even, there is an additional body centring, giving the bcc translational symmetry. If different rationals are used for the three internal components one can either have a tetragonal unit cell when two of the three rationals are equal, or an orthorhombic unit cell if all three rationals are different.

If one maintains the irrational value of the ϕ's occuring in the three external components the approximant structure will consist of the same two rhombohedra as the i-PT. On the contrary, if one also replaces the ϕ's occurring in the external components by rationals, for example such that the 6d lattice remains hypercubic, then the rhombohedra are deformed and more than two tiles occur. We will call these tilings deformed approximants.

Due to the scaling properties of i-PT's there is a very simple expression which gives approximately the number of vertices inside the unit cell for any perfect rational approximant, having either a cubic, an orthorhombic or a tetragonal unit cell, namely:

$$N(n) = N_0 \phi^n \tag{2}$$

where N_0 is a constant, and n a positive integer. For two successive cubic approximants the difference in the corresponding values of n is three. In the symmetrized approximants (see Sect.

2.2.2) vertices have been added or removed, so that this formula is somewhat less accurate. However it still gives a good indication on the number of vertices.

2.2.2 *Symmetrized tilings.* — In the calculation of vibrational spectra for clusters it is for computational reasons desirable to have a cluster which has perfect icosahedral symmetry (I_h). To achieve this, physical space V_E must pass through a position of the 6d periodic structure with sufficiently high site symmetry, i.e. a lattice point or a 6d body centre. As explained in section 2.1, this implies that there are boundary intersections, and we have to decide what to do with these. For instance, we could include all the boundary points in the atomic surfaces, or just a certain subset. In the latter case, this subset must have icosahedral symmetry. In either case we do not obtain the set of vertices of an i-PT. We can also construct tilings which have the symmetry of some subgroup of I_h, by choosing the appropriate set of boundary points to be included in the atomic surface.

The same holds for periodic approximant tilings. In general these have no (non-trivial) point symmetry, but by including (or excluding) all boundaries to the atomic surfaces T_h-symmetry (order 24) can be obtained in the case of an approximant with cubic lattice (the icosahedral group and the cubic group have T_h as a common subgroup). Again, the resulting structure is not the set of vertices of a tiling made by Penrose rhombohedra.

For the dynamical model to be considered we must take care that in the symmetrization process no 'too short distances' are produced, and that no sites occur which have too many or too few neighbours. This would indeed be the case for sites originating from a corner of an atomic surface. Therefore for the symmetrized tilings considered in this paper these corners were excluded, whereas the rest of the boundary was included.

Symmetrization is very useful if we want to consider larger systems. A non-trivial point group symmetry can be used to transform the dynamical matrix, which is of order three times the number of sites in the system, to block diagonal form, leaving us to solve the eigenvalue problem for a number of matrices of much smaller size. Each matrix block will give solutions which transform according to one of the irreducible representations of the symmetry group.

2.2.3 *Random tilings and randomized tilings.* — The term 'random tiling' [3, 4] refers to a statistical ensemble of tilings all made of the same two kinds of rhombohedra as the i-PT's. Any such tiling covering space with no overlap is in this ensemble, and all tilings in the ensemble have the same statistical weight. As it turns out, tilings which are nearly i-PT's are abundant in this ensemble. There are many more ways to build a tiling which is almost an i-PT than there are ways to build a periodic or more exotic tiling. Numerical simulations [4] indicate that if one picks at random a tiling from this ensemble one gets, with probability one, a tiling which resembles an i-PT. In this context, 'resembling' means the following. Any tiling made of the two rhombohedra can be lifted to a 3d lattice hypersurface in a 6d cubic lattice. The tiling is recovered by projecting this lattice surface, made of 3-facets of the 6d hypercubes, onto external space V_E. Apart from the choice of an origin, this lifting is unique. The lift of a true i-PT is a lattice surface which follows as closely as possible a 3-dimensional plane parallel to V_E. In the case of a general rhombohedral tiling more general lattice surfaces occur. However, with probability one a surface is obtained whose deviation from a plane parallel to V_E is uniformly bounded. Alternatively, a general rhombohedral tiling can be viewed as a wiggly cut through a 6d periodic structure, whereas true i-PT's correspond to plane cuts through the same periodic structure. Tilings whose lattice surface in the 6d lattice have a bounded deviation from a plane parallel to V_E are said to resemble an i-PT. In fact, they share many important properties with i-PT's. In particular, they have a Bragg component in their Fourier spectrum at the same positions as the i-PT, and may thus serve as a genuine model for quasicrystals.

Since a typical representative of a random tiling resembles an i-PT, it can be justified to pass to a subensemble of all tilings, namely to those tilings which have a given lattice periodicity. The same periodicity as for the commensurate approximant tilings will be used, which guarantees that the deviation from the full random tiling ensemble will be minimal, given the size of the unit cell. Passing to commensurate approximant random tilings has the advantages that it is easier to produce 'typical' representatives from this ensemble, and it will enable us to use periodic boundary conditions for the dynamical model to be considered below.

Representatives from the subensemble of random tilings with a given lattice periodicity can be obtained from commensurate approximant tilings by repeatedly flipping certain configurations of rhombohedra. There are sites which are corners of exactly four rhombohedra, two thick and two thin ones. These rhombohedra form a rhombic dodecahedron which can be filled in two different ways by the four rhombohedra. The flipping process consists of exchanging the filling of such a dodecahedron by its mirror image. This elementary process is used in a Monte Carlo algorithm: sites are repeatedly chosen at random, and each time one picks a site inside such a dodecahedron the flipping procedure is applied. It can be shown that this procedure satisfies detailed balance and is ergodic in the space of all rhombohedra tilings with a given lattice periodicity, thus providing a valid Monte Carlo algorithm. All representatives of random tilings considered in this paper have been produced by this algorithm. For further details concerning the algorithm we refer to Tang [4]. Since we will be able to use only some very few representatives in this paper and not the whole random tiling ensemble, and in view of the way these representatives are produced, we shall call them 'randomized tilings' from now on.

As explained above, randomized tilings can be represented by fluctuating 3D surfaces in a 6d cubic lattice. The degree of randomization is characterized by the roughness of these surfaces. More precisely, if we denote by $\mathbf{h}$ the internal space coordinates of each site, the randomness of the tiling can be monitored by the average phason strain, defined by $< \mathbf{h}^2 > - < \mathbf{h} >^2$, where the average $< \cdot >$ is taken over all atoms in one unit cell. The average phason strain has a value of about 1.25 for a perfect approximant tiling, and increases rapidly with randomization up to about 1.73, where it saturates for a completely randomized tiling of infinite size. Due to finite size corrections, we can expect a value of 1.58 for a fully randomized 3/2-approximant [4].

2.3 DYNAMICAL MODEL. — The dynamical model we consider consists of atoms placed on the vertices of the tiling which interact with their neighbours. As neighbours in the i-PT and the non-deformed approximants we have taken all pairs of atoms with neighbouring distance equal to $\sqrt{6-3\phi}$ (≈ 1.070), $\sqrt{2+\phi}$ (≈ 1.902) or 2. The latter two distances are respectively the edges and the face diagonals of the rhombohedra and occur much more frequently than the shortest one, which is the body diagonal of the thin rhombohedron. In the symmetrized tilings one additional short distance equal to $2\phi - 2$ (≈ 1.236) occurs. In the deformed approximants the neighbour distances are slightly changed, and more than three (or four in the symmetrized case) short distances occur. However in the limit of large unit cells these distances converge to the three or four distances mentioned above. Connecting nearest neighbours by springs leads to the following expression for the potential energy:

$$\Phi = \frac{1}{4} \sum_i \sum_{i'(i)} \alpha_{ii'} [|\mathbf{r}_i + \mathbf{u}_i - \mathbf{r}_{i'} - \mathbf{u}_{i'}| - |\mathbf{r}_i - \mathbf{r}_{i'}|]^2 \tag{3}$$

where the summation $\sum_{i'(i)}$ runs over all neighbours of i, $\alpha_{ii'}$ is the spring constant of the spring between atom i and i' and $\mathbf{u}_i$ the displacement of atom i relative to its equilibrium position

$\mathbf{r}_i$. The strength of the spring constants can be varied according to the bond length. Although the density of states changes when the spring constants are varied, as is shown in reference [1], the scaling behaviour of the spectrum and the character of the eigenvectors turn out to be qualitatively independent of choice of the spring constants. Since we are primarily interested in the consequences of the special topology of our model tilings for the lattice dynamics, the same spring constant was taken for all neighbouring pairs in a given tiling, although this spring constant may vary somewhat from tiling to tiling.

In the harmonic approximation, where all terms of order three and higher in the Taylor expansion for small displacements are neglected, the consequence of the choice of the potential (3) is that only the distortion of the spring parallel to $\mathbf{r}_{ii'}$ is taken into account, where $\mathbf{r}_{ii'}$ is the vector connecting the equilibrium positions of the atoms i and i'. So in fact we can replace (3) by:

$$\Phi = \frac{1}{4}\sum_i \sum_{i'(i)} \alpha_{ii'} u_{ii',\parallel}^2 \tag{4}$$

where $\mathbf{u}_{ii',\parallel} = \mathbf{u}_{i,\parallel} - \mathbf{u}_{i',\parallel}$. For almost all the results presented in this paper this potential is used. However to illustrate how sensitive the model is to changes of the potential we will present one result where besides a parallel term also a perpendicular term is taken into account:

$$\Phi = \frac{1}{4}\sum_i \sum_{i'(i)} [\alpha_{ii'} u_{ii',\parallel}^2 + \beta_{ii'} u_{ii',\perp}^2] \tag{5}$$

The second term has a physical justification in the fact that atoms do not only interact with the hard cores of neighbouring atoms but also with the surrounding electrons, so that the potential will in general not be spherically symmetric, which is implicitly assumed in the potential (3), since this potential only depends on the absolute values of the difference vectors $\mathbf{u}_{ii'}$.

In the harmonic approximation the equation of motion is given by:

$$m_j \ddot{u}_{j\alpha} = -\sum_{j'\alpha'} \Phi^{(2)} \begin{pmatrix} j & j' \\ \alpha & \alpha' \end{pmatrix} u_{j'\alpha'} \tag{6}$$

where $\Phi^{(2)}$ is the matrix containing the second order partial derivatives with respect to the displacements. For simplicity we choose from now on the masses m_j equal to 1. Substituting this and $u_{j\alpha} = c_{j\alpha} e^{i\omega t}$ into (6) leads to the following eigenvalue problem:

$$\omega^2 c_{j\alpha} = \sum_{j'\alpha'} \Phi^{(2)} \begin{pmatrix} j & j' \\ \alpha & \alpha' \end{pmatrix} c_{j'\alpha'} \tag{7}$$

For the i-PT this eigenvalue problem is infinite. For a cluster however, either with fixed or clamped boundary conditions, it becomes finite. For a commensurate approximation the lattice periodicity is recovered and one can apply normal lattice dynamics using Bloch waves. The dynamical matrix can then be decomposed into finite dimensional blocks each of them corresponding to a certain wave vector $\mathbf{k}$.

3. Density of states.

The deformed symmetrized 1/1-approximant, resulting from a 6-dimensional cubic structure, turns out to be an ordinary 3-dimensional fcc-structure, having one atom in the primitive cell. In a dynamical model where each atom is connected to its 12 nearest neighbours by springs of

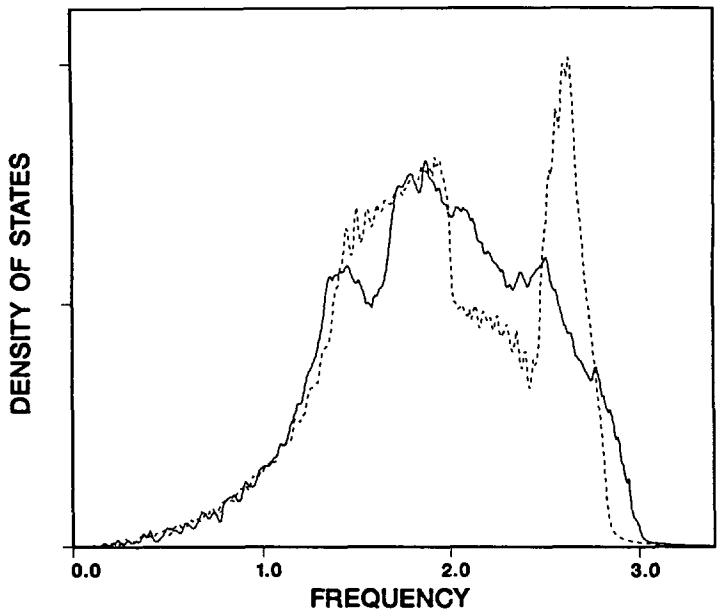

Fig.1. — The normalized density of states for the symmetrized 5/3-approximant (solid curve) and an fcc-structure (dotted curve), using a similar number of states and an equal 'mean spring force' per atom.

equal strength ($\alpha_{ii'} = 1$) the DOS has two sharp peaks, one at $\omega = 1.9$, due to the transversal branches, the other at $\omega = 2.6$, due to the longitudinal branch. This is illustrated in figure 1 (dashed curve). The same picture also shows the DOS for the deformed symmetrized 5/3-approximant, with 2530 atoms per unit cell (solid curve). In the latter case only the states belonging to **k**-values with high symmetry were considered, i.e. $\mathbf{k} = (0,0,0)$, $\mathbf{k} = \pi/a(1,1,1)$, $\mathbf{k} = \pi/a(1,0,0)$ and $\mathbf{k} = \pi/a(1,1,0)$, where a is the size of the cubic unit cell. The first two k-vectors have weight one and yield complete T_h-symmetry of order 24, whereas the latter two have weight three and yield D_{2h}-symmetry of order 8. The **k**-vectors yielding D_{2h}-symmetry belong to an orbit of three symmetry equivalent vectors inside the irreducible part of the Brillouin zone, and so the states belonging to these vectors have to be counted three times to obtain the correct DOS. For the fcc-structure **k**-vectors lying on a whole grid in the Brillouin zone were considered. The curves were determined by using the following expression:

$$D(\omega) = \frac{1}{\pi}\mathrm{Im}\sum_i \frac{1}{\omega - \omega_i - i\epsilon} \tag{8}$$

where ϵ was taken equal to 0.01. This expression is especially useful to obtain a slightly smoothed DOS when only a limited number of eigenstates is available. In both cases the DOS was normalized such that the aera enclosed is equal to 1. Unlike in the fcc-case, in the 5/3-approximant atoms can have different neighbour configurations. In order to make a 'correct' comparison, the strength of the spring constants was chosen such that the 'mean spring constant' per atoms is equal in both cases:

$$\frac{1}{N}\sum_i \sum_{i'(i)} \alpha_{ii'} = 12 \tag{9}$$

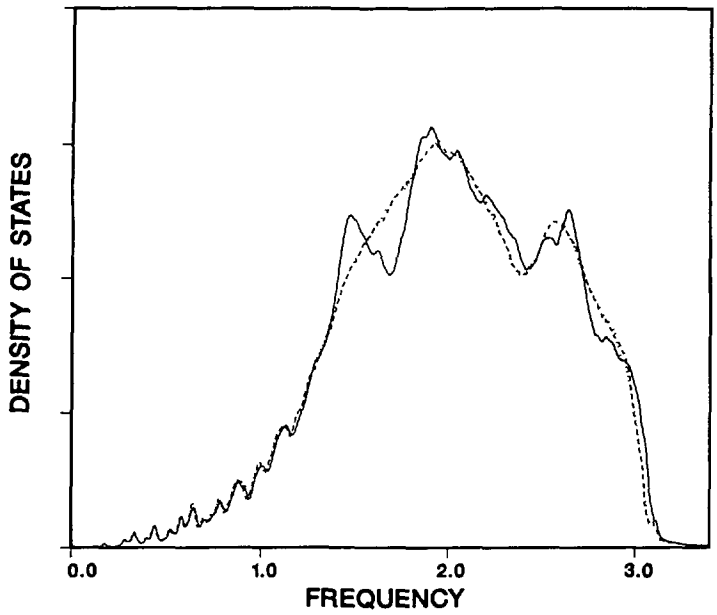

Fig.2. — The density of states for a tetragonal approximant of the i-PT with 932 atoms in the unit cell (solid curve) and two randomized versions for this approximant (dotted curve and dashed curve).

where N is the number of atoms in the unit cell. For the 5/3-approximant, where the mean number of neighbours per atom is 13.69, the spring constant therefore was taken equal to $\alpha_{ii'} = 12./13.69$ for all neighbouring atoms i and i'.

Figure 1 shows that the strong peaks have disappeared for the 5/3-approximant, and are replaced by weaker ones. This can be understood by observing that the three branches causing the strong singularities in the fcc-case have been replaced 3×2530 branches in the relatively small Brillouin zone of the 5/3 unit cell, which yields much weaker singularities. The relatively smooth behaviour of the DOS was also found experimentally by doing inelastic neutron-scattering experiments on icosahedral PdSiU [9]. Another point to mention is that the upper bound of the spectrum (cut-off frequency) is shifted somewhat to the right, an effect which was also observed for the Fibonacci chain [5]. At low frequencies there is a global ω^2-behaviour with about the same proportionality constant in both cases. However, in the 5/3-approximant there seems to be some clustering of eigenfrequencies, at least more than in the fcc-case. A detailed numerical analysis of the low frequency region is in progress.

To study the effect of randomization on the DOS we have taken a approximant with a tetragonal unit cell containing 932 atoms. In figure 2 the normalized DOS is shown for the perfect approximant (solid line) and two randomized versions of it (dashed and dotted line). Again only the eight special k-values yielding real dynamical matrices were considered. All spring constants were taken equal to 1. One observes that randomization induces a smoothing of the DOS, and that the first peak completely disappears. There is little difference between the curves belonging to different randomized approximants, which suggests that these curves are characteristic for randomized tilings. At low frequencies there is hardly any difference visible between all three curves. Obviously the accoustic modes are not affected by changes in the fine structure.

To determine the sensitivity of the density of states to the kind of potential that is used, we

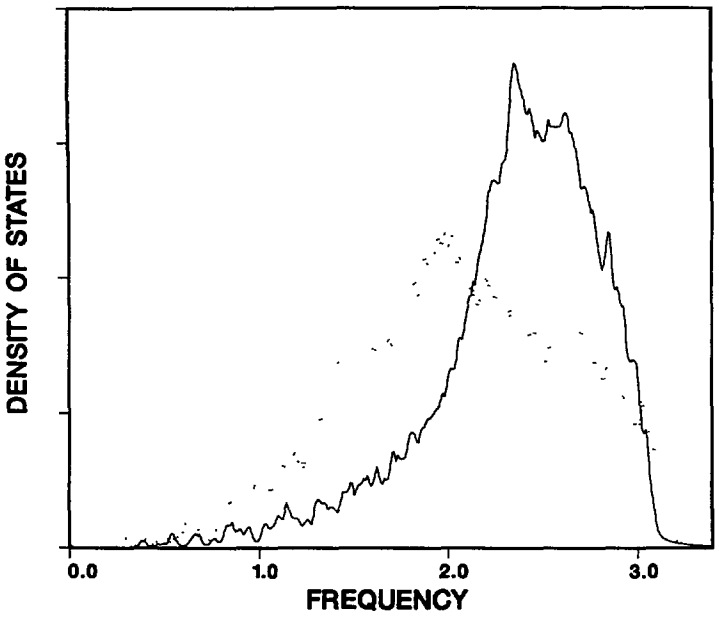

Fig.3. — The density of states for the deformed symmetrized 3/2-approximant using the potential (5) with $\alpha_{ii'} = 3/4$ and $\beta_{ii'} = 1/4$ for each neighbour pair (solid line). The dotted line gives the result for $\alpha_{ii'} = 1$ and $\beta_{ii'} = 0$.

have calculated the DOS for the deformed symmetrized 3/2-approximant (599 atoms) using the potential (5), with $\alpha_{ii'} = 3/4$ and $\beta_{ii'} = 1/4$ for each neighbouring pair. The result is shown in figure 3 (solid line), and compared with the result for the case where $\alpha_{ii'} = 1$ and $\beta_{ii'} = 0$ (dotted line). It appears that the DOS is indeed sensitive to the kind of potential. However, for a qualitative study of the spectrum relative to the spectrum of a simple periodic structure this dependence on $\alpha_{ii'}$ and $\beta_{ii'}$ is not very important. Also, a value of $\beta_{ii'}$ equal to one third of the value of $\alpha_{ii'}$ is probably unrealistically large. In our study of the eigenvectors we encountered no qualitative dependence on the perpendicular term in the potential. Therefore, in the following we always take $\beta_{ii'} = 0$.

4. Scaling behaviour of the spectrum.

The rational approximants of the i-PT are related to each other by scale transformations, just as for the Fibonacci chain. For the Fibonacci chain as well as for other 1-dimensional incommensurate systems it was shown that also the band structure of phonon and tight binding models have certain scaling properties. To study the scaling behaviour of spectra we used a multifractal analysis of the bandwidths, suggested by Kohmoto for spectra in 1-dimensional systems. Doing this numerically for several successive rational approximants one might be able to derive the scaling behaviour of the bandwidths in the incommensurate limit.

First we give a generalization of Kohmoto's method for systems in arbitrary dimension. Define a measure L for the size of the system by:

$$L = (sN)^{(1/s)} \tag{10}$$

where s is the dimension of the system and N the number of atoms inside the unit cell, so that

sN is equal to the number of branches. For each band define a scaling index ϵ_i, by:

$$\Delta_i = (1/L)^{\epsilon_i} \tag{11}$$

where Δ_i is the width of the i-th branch. A definition of the bandwidth for a 3-dimensional branch will be given later. Furthermore an 'entropy' function $S(\epsilon)$, representing the distribution over the ϵ_i is defined by:

$$\Omega(\epsilon) = L^{S(\epsilon)} \tag{12}$$

where $\Omega(\epsilon)\mathrm{d}\epsilon$ is the number of branches with scaling index between ϵ and $\epsilon + \mathrm{d}\epsilon$. Suppose now that we are enlarging the system in steps, such that the number of branches at the n^{th} step is approximately given by $sN = Cr^n$, where $C > 0$ and $r > 1$ are constants (in our case we will have $r = \phi^3$). If in the limit of large n all bandwidths scale proportionally to $1/L$ the spectrum is absolutely continuous, and the support of the S-function is just one point, i.e. $\epsilon = 1$ and $S(1) = s$. In the case where all bandwidths decay exponentially in n, as $\exp(-\gamma n)$, but with constants γ depending on the band, one finds a distribution of finite scaling indices, and the support of the S-function is not just one point. Such a spectrum is called singularly continuous. Finally, if all bandwidths decay faster than exponentially in n, for example as $\exp(-\gamma L)$, then the spectrum is a pure point spectrum, with all scaling indices tending to infinity, so that $S(\infty) = s$.

Numerically one could calculate the distribution $\Omega(\epsilon)$ by first determining the value of $\Omega(\epsilon)\Delta\epsilon$, simply by counting the number of branches with a scaling index between ϵ and $\epsilon + \Delta\epsilon$, and then dividing this by $\Delta\epsilon$. However, $\Omega(\epsilon)$ can be a very irregular function, so that the computed result strongly depends on the choice of the interval $\Delta\epsilon$. Therefore the 'entropy', which is in fact the function we are interested in, is calculated by using the following thermodynamical formalism. Define a 'partition function' by:

$$Z(\beta) = \sum_{i=1}^{sN} \Delta_i^{\beta} \tag{13}$$

and a 'free energy' as:

$$F(\beta) = \frac{\ln Z(\beta)}{\ln(L)} \tag{14}$$

Then the functions $S(\epsilon)$ and $F(\beta)$ are related by the following Legendre tranformation:

$$S(\epsilon) = F(\beta) + \beta\epsilon \tag{15}$$

with:

$$\epsilon = -\frac{\mathrm{d}F(\beta)}{\mathrm{d}\beta} \tag{16}$$

In the application of this analysis to the spectra of rational approximants of the i-PT we use the following definition of bandwidth:

$$\Delta_i = \max_{j,j'=1,8} |\omega_i(\mathbf{k}_j) - \omega_i(\mathbf{k}_{j'})| \tag{17}$$

where i is the branch label, and $\mathbf{k}_j$ ($j = 1, 8$) are the eight $\mathbf{k}$-vectors mentioned above. Although in general these bandwidths are not the true bandwidths they can very well be used for the purpose of studying the scaling behaviour of the bandwidths under scale transformations where

the system is enlarged in three directions. Care must be taken with the definition of bandwidth if, for example, one has to study the scaling behaviour of the spectrum for 3-dimensional systems under scale transformations in one or two directions (e.g. in the decagonal phase). In that case one has to define a bandwidth (or projected bandwidth) respectively on a line or in a plane in the Brillouin zone.

Figure 4a shows the S-function for the deformed symmetrized 2/1-, 3/2- and 5/3-approximants, having respectively 135, 599 and 2530 atoms inside the unit cell. The differences in mean number of neighbours (13.60, 13.82 and 13.69, respectively) were compensated by choosing an appropriate spring constant for each of the three systems (13.69/13.60, 13.69/13.82 and 1, respectively). From this picture one can not yet conclude that the spectrum of the i-PT is singularly continous, because the infinite limit has not been reached and complete convergence is not observed yet. In fact one sees that the lower bound of the support of the S-function is shifted to the right when the system is enlarged. The low ϵ-values correspond to branches with large bandwidths, which are the lower (accoustic) branches. This is illustrated in figure 5 for the 2/1-approximant, where the bandwidths are indicated by the horizontal bars, at frequencies corresponding to the centres of the branches. Having observed (in Fig. 4a) that the ϵ-values corresponding to the lower branches are slightly shifted towards the value $\epsilon = 1$ we suspect that these branches scale as in an absolutely continuous spectrum. Whether this is true can numerically be checked as follows.

Suppose that for a system of dimension s the bandwidths scale as if they belong to a absolutely continuous spectrum. Then one can write:

$$\Delta_i = \frac{c_i}{L} \tag{18}$$

Now we can enlarge the system in s directions by replacing one unit cell by K^s unit cells, where K is an integer for the moment. We now determine the relation between the S-functions of the band spectrum corresponding to this enlarged unit cell and the original unit cell. Assuming that all branches depend only linearly on the wave vector $\mathbf{k}$ the relation (18) holds for all i and the 'partition function' for the enlarged system becomes:

$$Z'(\beta) = \sum_{i=1}^{sN} K^s \left(\frac{\Delta_i}{K}\right)^\beta \tag{19}$$

and the 'free energy':

$$F'(\beta) = (s-\beta)\frac{\ln(K)}{\ln(KL)} + \frac{\ln(Z)}{\ln(KL)} = (s-\beta)\frac{\ln(K)}{\ln(KL)} + \frac{\ln(L)}{\ln(KL)}F(\beta) \tag{20}$$

For ϵ' one finds:

$$\epsilon' = -\frac{\mathrm{d}F'(\beta)}{\mathrm{d}\beta} = \frac{\ln(K)}{\ln(KL)} + \frac{\ln(L)}{\ln(KL)}\epsilon \tag{21}$$

and for the 'entropy function':

$$S'(\epsilon') = F'(\beta) + \beta\epsilon' = (s-\beta)\frac{\ln(K)}{\ln(KL)} + \frac{\ln(L)}{\ln(KL)}(S(\epsilon) - \beta\epsilon) + \beta\epsilon' \tag{22}$$

With the expressions (21) and (22) one is able to calculate, starting from a set $(\epsilon_i, S(\epsilon_i))$ corresponding to a system of size L, the set $(\epsilon_i', S'(\epsilon_i'))$ for a system of size KL. These expressions show clearly that in the limit of $K \to \infty$ the value of ϵ' converges to 1 with $S'(1) = s$, as it should be for an absolutely continuous spectrum. Although K has to be an integer from

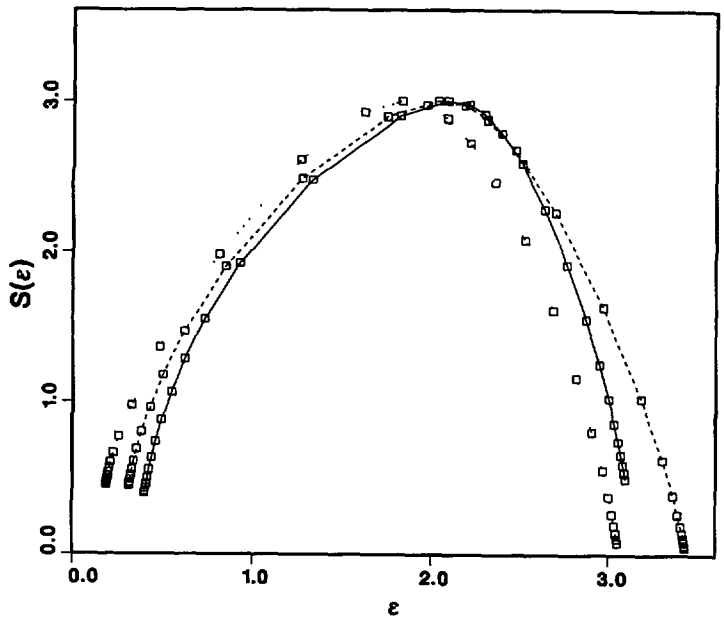

a)

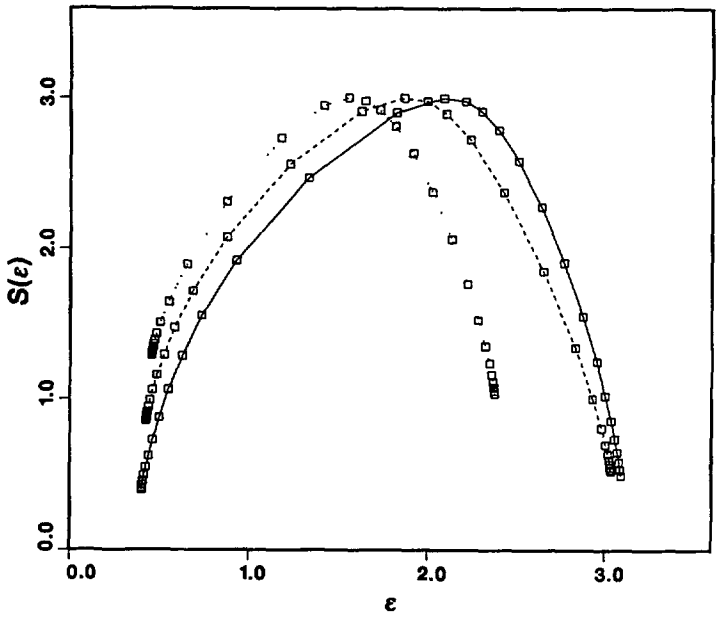

b)

Fig.4. — a) The spectral S-function for the deformed symmetrized 2/1-,3/2- and 5/3-approximants (dotted, dashed and solid line, respectively). b) Same as in figure 4a, but now for systems of equal 'size'.

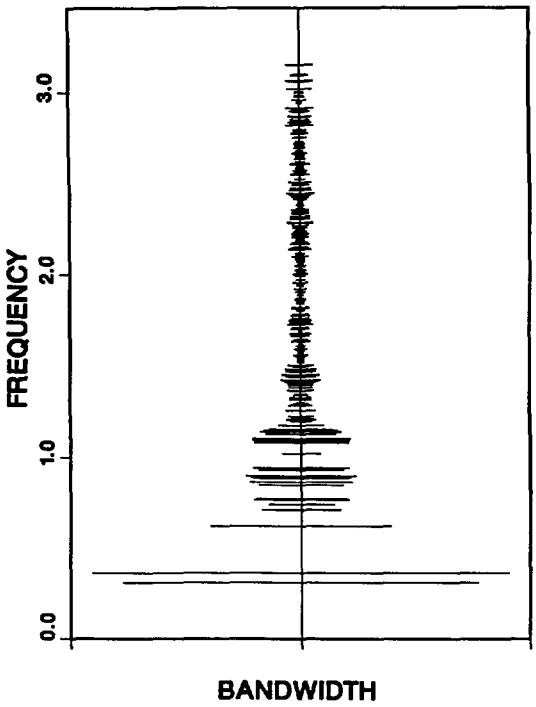

Fig.5. — The relative bandwidths for the symmetrized 2/1-approximant, represented by horizontal lines at vertical positions corresponding to the centers of the branches. The units on the horizontal axis are arbitrary.

a physical point of view one can make an analytic continuation permitting also non integer values. In this way we are able to 'renormalize' the S-function to a system of arbitrary 'size'. By making use of this we can compare the spectral S-functions for two different systems at equal 'size', even if the numbers of atoms in the primitive unit cells are mutually prime.

Figure 4a presents the results for systems of 'sizes' that correspond to the number of atoms inside the primitive cubic unit cell for the 2/1- and 3/2-approximant, and to the smallest cubic unit cell for the 5/3-approximant (which is non-primitive). Applying the 'renormalization' both to the 2/1- and to the 3/2-approximant leads us to figure 4b, where the 'size' of the systems for these two approximants was taken equal to the 'size' of the 5/3-approximant (with $N = 2530$). This picture shows that the minimal values of ϵ ($\epsilon_{\min}$) are almost the same in all three cases, which means that the scaling behaviour of the largest bands is close to that of an absolutely continuous spectrum. On the other hand the value of $S(\epsilon)$ at $\epsilon_{\min}$ decreases for the higher approximants. Obviously there is a decrease of the low frequency range where the behaviour of the spectrum is close to absolutely continuous. In the limit this region might even converge to just one point, i.e. $\omega = 0$. At large ϵ-values the difference from an absolutely continuous behaviour is more pronounced.

In order to have a reference a comparison is made with the results for the Fibonacci chain. Figure 6a shows the spectral S-function for three rational approximants of the Fibonacci chain. The approximants are separated by three inflation steps and have unit cells of 34, 144 and 610 atoms, respectively. In figure 6b the result is shown for the same three approximants, but

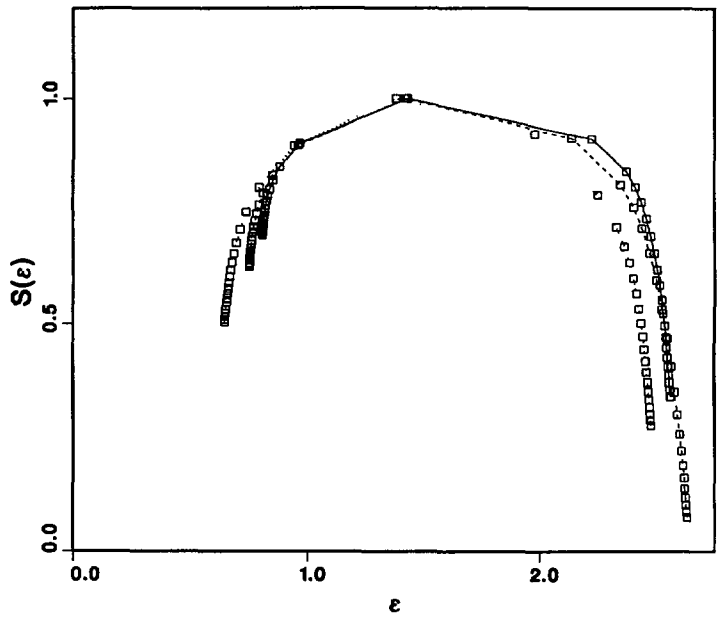

a)

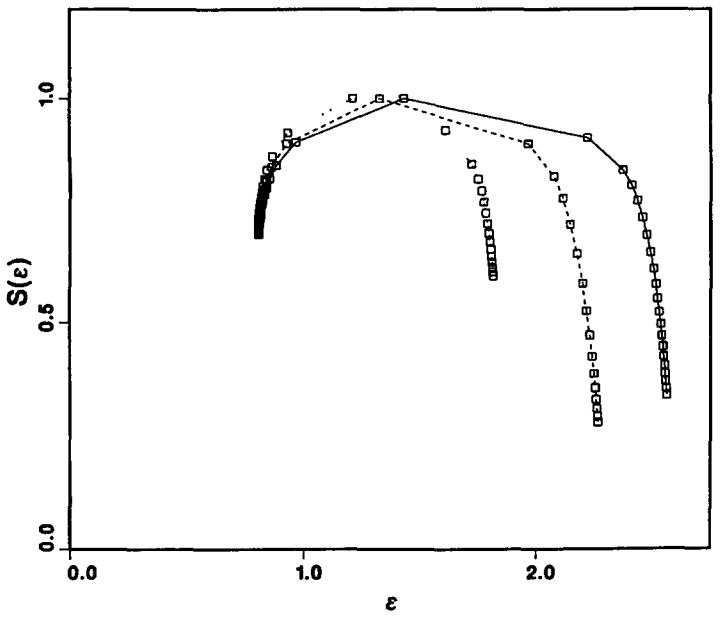

b)

Fig.6. — a) The spectral S-function for three rational approximants of the Fibonacci chain having respectively 34 (dotted line), 144 (dashed line) and 610 (solid line) atoms in the unit cell. b) Same as in figure 6a, but for systems of equal 'size'.

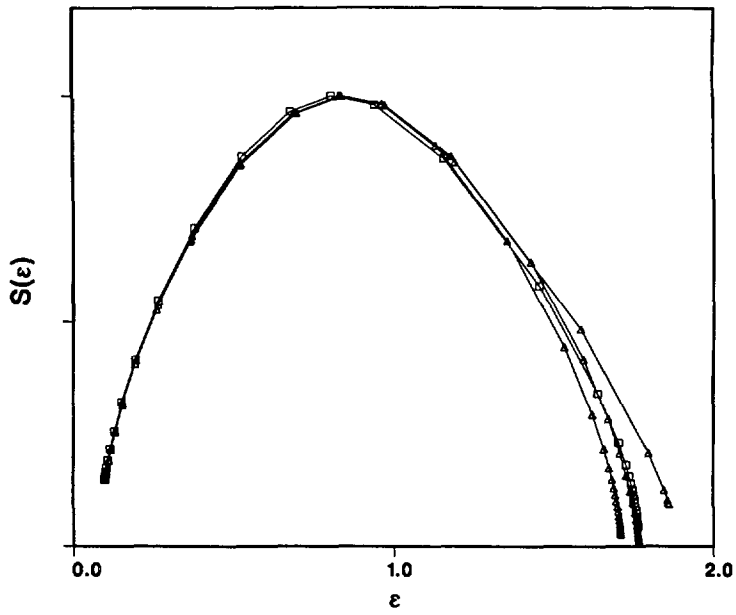

Fig.7. — The spectral S-function for a perfect 3/2-approximant (square marks) and three randomized configurations of this approximant (triangular marks).

now the 'size' of the systems is taken equal to the 'size' of the 610-approximant in all three cases. Qualitatively we see a similar behaviour as in figure 4b. At ϵ_{min} the value of $S(\epsilon)$ decreases for the higher approximants, but not as much as for the i-PT approximants, and therefore is hardly visible. Comparing figures 4 and 6 it seems that the scaling behaviour of the spectrum for the i-PT approximants is not less singularly continuous than for the Fibonacci chain approximants, for which it has been shown analytically that the spectrum is singularly continous [5, 6]. However, one should recall that only three relatively small i-PT approximants have been considered, so that it might be too early to draw any final conclusions. Due to computer limitations, we have not been able to do these computations for larger approximants. For the symmetrized 8/5-approximant most irreducible matrix blocks are already of the order of about 4000, and the computation time needed for eigenvalue routines is proportional to the cube of the order of the matrix, not to mention the storage capacity that is required.

Qualitatively there is hardly any difference between the spectral S-functions for perfect and randomized approximants. This is shown in figure 7 where the S-function is given for the perfect 3/2-approximant (square marks) and three randomized 3/2-approximants (triangular marks). The accoustic part (i.e. at low ϵ) is hardly affected, as expected, and at high ϵ there are only small deviations, but not in a particular direction. This means that it is likely that the spectral scaling behaviour for randomized approximants is very similar to the behaviour for perfect (or symmetrized) approximants, and thus that the character of the spectrum for the respective limit tilings is the same.

5. Character of the eigenvectors.

A measure for the number of atoms participating to a certain eigenmode is given by the participation fraction (PF), which is defined by:

$$\mathrm{PF} = \frac{1}{N \sum_{i=1}^{N} p_i^2} \tag{23}$$

where N is the number of atoms, $p_i = |\mathbf{u}_i|^2$ with $\mathbf{u}_i$ the displacement of atom i from its equilibrium position, assuming a normalized state, i.e. $\sum_{i=1}^{N} p_i = 1$. This is a natural definition: if M of the p_i's are equal to $1/M$, and the other p_i's vanish, then we obtain indeed $\mathrm{PF} = M/N$. In particular, the PF has the value 1 if all p_i are equal, and it is equal to $1/N$ if only one atom participates in the eigenmode.

In the presence of degeneracy the eigenvectors are not uniquely determined. In particular the values of the PF for two modes at $\mathbf{k}$ and $-\mathbf{k}$ depend on the choice that is made for the two eigenvectors, spanning the twofold degenerated eigenspace. So first we specify this choice.

The real displacements of the atoms for an eigenmode in a lattice periodic structure with wave vector $\mathbf{k}$ and frequency ω can be given by:

$$u_{\mathbf{n}j} = u_{0j} e^{i(\mathbf{kn} - \omega t)} + cc \tag{24}$$

where j labels the atoms inside the unit cell, $\mathbf{n}$ is a lattice vector and $u_{\mathbf{n}j}$ the real displacement of atom j in the unit cell at position vector $\mathbf{n}$. Generically this represents a travelling wave solution and, except for the special $\mathbf{k}$-vectors that yield a real dynamical matrix, there will be a solution at $-\mathbf{k}$ with the same frequency travelling in the opposite direction. These two solutions can be combined to two standing wave solutions. For the exceptional $\mathbf{k}$-vectors yielding a real dynamical matrix, i.e. those which satisfy $\mathbf{kn} = m\pi$ for all lattice vectors $\mathbf{n}$, with m some integer (depending on $\mathbf{n}$), the solution (24) already represents a standing wave. In this case the solution at $-\mathbf{k}$ is identical, since for such wave vectors we have $-\mathbf{k} = \mathbf{k} + \mathbf{K}$, with $\mathbf{K}$ a reciprocal lattice vector. Other degeneracies can occur for example due to some point group symmetry, or as a consequence of not using a primitive unit cell. For the results to be unique it is preferable to avoid degeneracies as much as possible, and therefore one should do the calculations using a primitive unit cell. In our calculations for the i-PT approximants and the Fibonacci chain this is what we did, except for the 5/3-approximant where we used the smallest cubic unit cell, whereas the primitive cell is a bcc cell.

After this intermezzo we come back to the definition of the p_i's and conclude that it makes a difference whether one considers standing or travelling waves. Since for certain $\mathbf{k}$-vectors there exist only standing waves we define the p_i's as the squared amplitudes of the atoms in standing waves. This means that in general one cannot normalize a state over one primitive unit cell. Instead, a larger unit cell is required for the normalization, such that the half wave length of the eigenmode fits into it. For the Brillouin zone corresponding to this large unit cell the eigenmodes belong to one of the wave vectors that yield a real dynamical matrix.

As an example let us consider the PF for eigenmodes in a mono-atomic chain. The real displacements of the atoms are given by $A\cos(kna)$, where A a normalization constant, k the wave number, n an integer label for the lattice sites and a the size of the primitive unit cell. The values of k can be chosen inside the Brillouin zone $(-\pi/a, \pi/a]$. It can easily be shown analytically that the PF takes the value 2/3 for all k-values, except for $k = 0$ and $k = \pi/a$, for which $\mathrm{PF} = 1$, and $k = \pi/2a$, for which $\mathrm{PF} = 0.5$.

Likewise, for a 3-dimensional fcc structure (having one atom in the primitive unit cell) analytically one finds that the PF will take the values 1 and 0.5 for certain special wavevectors. For all other $\mathbf{k}$-vectors PF is equal to 2/3.

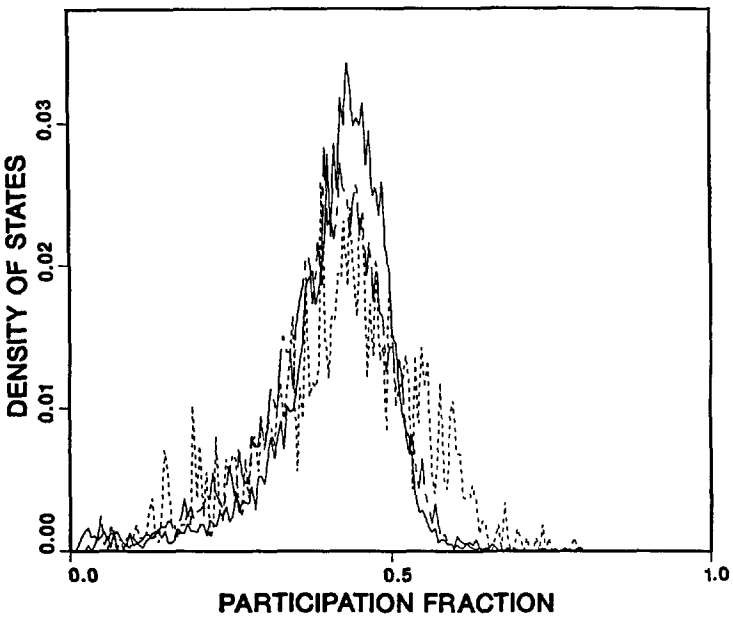

Fig.8. — The density of states as a function of the participation fraction for the symmetrized 2/1-, 3/2- and 5/3-approximants (dashed, chaindashed and solid lines, respectively).

The PF is defined for each eigenmode, so that one can study the density of states as a function of PF. In figure 8 the DOS is presented for three symmetrized i-PT approximants, showing that the average PF is considerably lower than 2/3. One also observes that the average PF is not decreasing when tending to higher approximants, which means that for most states localization is not enhanced as we approach the incommensurate limit. Figure 9 shows the DOS as a function of PF for a perfect and two randomized 932-approximants (with same configurations as in Sect. 2). The first conclusion we draw from this picture is that, for the majority of the states, localization is not enhanced by randomization, but rather the contrary, since the peaks for the randomized cases are shifted slightly to higher values of the PF. Considering what is known about random systems in one and two dimensions, this is not what we expected. A possible explanation for this phenomenon might be that the randomized configurations have a more homogeneous connectivity distribution. This can be analyzed as follows. Let γ_i be the number of neighbours of atom i and let $< \gamma >$ be the average number of neighbours per atom. A measure for the variation around the mean value is given by the standard deviation, which is defined by:

$$\Delta\gamma = \sqrt{< \gamma^2 > - < \gamma >^2} \tag{25}$$

where $< \gamma^2 >$ is the average of the squared number of neighbours per atom. These values, together with γ_{max} and γ_{min}, which are respectively the maximal and minimal number of neighbours of an atom occurring in the tiling, are listed in table I for the fcc structure, the symmetrized 2/1-,3/2- and 5/3-approximant, the perfect and the two randomized 932-approximants.

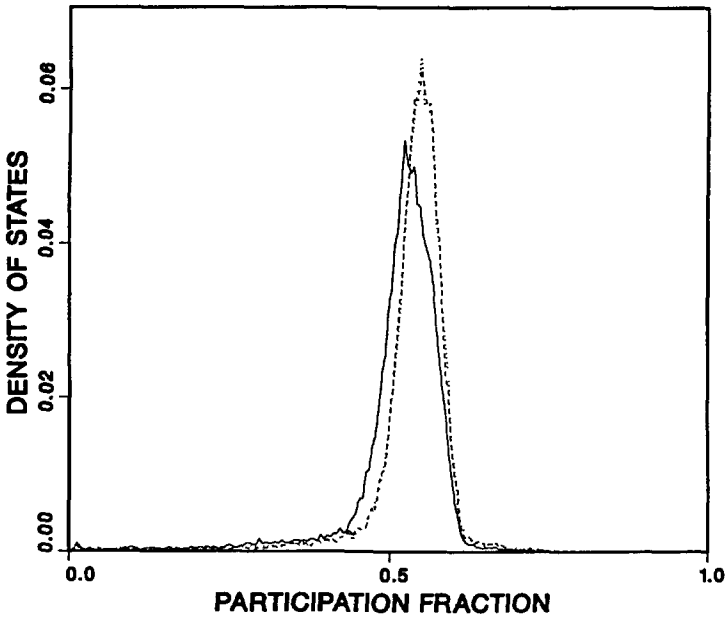

Fig.9. — The density of states as a function of the participation fraction for the perfect 932-approximant (solid line) and two of its randomizations (dashed and dotted line).

Table I.

	$<\gamma>$	$\Delta\gamma$	γ_{max}	γ_{min}
fcc	12.00	0.00	12	12
sym. 2/1-appr.	13.60	1.31	17	12
sym. 3/2-appr.	13.82	1.40	18	11
sym. 5/3-appr.	13.69	1.46	19	11
perf. 932-appr.	13.23	1.28	19	11
rand. 932-appr.	13.13	1.13	18	11
rand. 932-appr.	13.11	1.14	17	11

From this table we see that $\Delta\gamma$ for the two randomized 932-approximants is indeed smaller than for the perfect one, which means that in these tilings the distribution of coordination number is narrower, in a certain sense closer to the fcc case, which might explain why for the randomized configurations the PF distribution is narrower and shifted to the right (Fig. 9). However, comparing the result for the symmetrized 2/1-approximant in figure 8 with that of the perfect 932-approximant we observe a considerable shift while the difference in the standard deviation of the coordination is only very small. Here the explanation could be found in the symmetrization which induces an extra short neighbour distance and leads to an consirable structural change, especially for this low approximant.

We have also studied the PF as a function of frequency. However, since most of the states appeared to have a rather high PF, and only a few states have a considerably lower PF, the PF *versus* frequency plots are not very informative. Therefore we chose to present the inverse participation fraction (IPF), which is equal to 1/PF. Studying the IPF as a function of frequency for clusters with free or clamped boundary conditions and for all kinds of rational

approximants we found very similar results. In figure 10a, 10b and 10c the results are shown for, respectively, a symmetrized cluster (7895 atoms) with free boundary conditions, the symmetrized 5/3-approximant and a randomized tetragonal 932-approximant. In each case only the modes at the very upper end of the spectrum have a relative high IPF, i.e. are more localized.

Just as for the spectrum one can study the scaling behaviour of the eigenstates under systematic enlargement of the system, tending to the quasiperiodic limit, by a multifractal analysis. The method was introduced and used by Kohmoto for 1-dimensional systems, but can be used for systems in two or three dimensions as well. For each p_i a scaling index α_i is defined by:

$$p_i = (\frac{1}{L})^{\alpha_i} \tag{26}$$

where now $L = N$ is the number of atoms in the system, which is a good measure for the 'size' of the system. The partition over the α_i's can be represented by the 'entropy' function $S(\alpha)$, which is defined by:

$$\Omega(\alpha) = L^{S(\alpha)} \tag{27}$$

where $\Omega(\alpha)\mathrm{d}\alpha$ is the number of sites with scaling index between α and $\alpha + \mathrm{d}\alpha$. The $S(\alpha)$-function is calculated using the same thermodynamical formalism as the spectral $S(\epsilon)$-function, only with Δ_i replaced by p_i and ϵ by α.

Consider again the mono-atomic chain mentioned above. Taking a standing wave with rational wave number $k = \frac{m}{M}\frac{\pi}{a}$, so that it can be normalized with a 'size' of the system equal to $N = KM$ (K integer), the numbers p_n (n = 0, 1, . , N-1) for a normalized state are given by:

$$p_n = \frac{2}{N}\cos^2(\frac{nm}{M}\pi + \vartheta) \tag{28}$$

where ϑ is an arbitrary phase. The corresponding scaling indices α_n then become:

$$\alpha_n = 1 - \frac{\ln(2\cos^2(\frac{nm}{M}\pi + \vartheta))}{\ln(N)} \tag{29}$$

For sites with $p_n = 0$ the scaling index α_n is undefined, so that such sites have to be excluded from the partition sum in the thermodynamical formalism. Alternatively, the phase ϑ could be chosen such that no sites with $p_n = 0$ occur. For any fixed wave number k the numerator in (29) takes only finitely many different values, so that it is bounded from above and below. In the limit $N \to \infty$ all scaling indices α_n therefore tend to 1, which shows that for extended states in a periodic 1-dimensional system the support of the $S(\alpha)$-function consists of just one point, $\alpha = 1$, with $S(1) = 1$. This also holds true for all states in 2- and 3-dimensional periodic systems. It should be mentioned, however, that in practical cases, since one can only handle systems of finite size, the upper bound of the support of the $S(\alpha)$-function may converge very slowly to the value 1 for certain states, due to the fact that in standing waves there can be sites which are close to the nodes of the wave. On such sites p_n is very small, and thus α_n is large. On the other hand, the lower bound of the support of the $S(\alpha)$-function for such states typically converges much faster to the value 1, with correspondingly $S(1) = 1$. It is therefore this convergence which should be used as a criterion for a state to be extended. This criterion also leads us to the choice of the moment μ (see below). For localized states, which can only occur in aperiodic systems, one has $S(\alpha)$ equal to 0 at $\alpha = 0$ and $S(\alpha) = 1$ for α tending to infinity.

In the application of this analysis to the cubic i-PT approximants the 'size' of the system can be taken equal to the number of atoms inside the cubic unit cell. For the special **k**-vectors

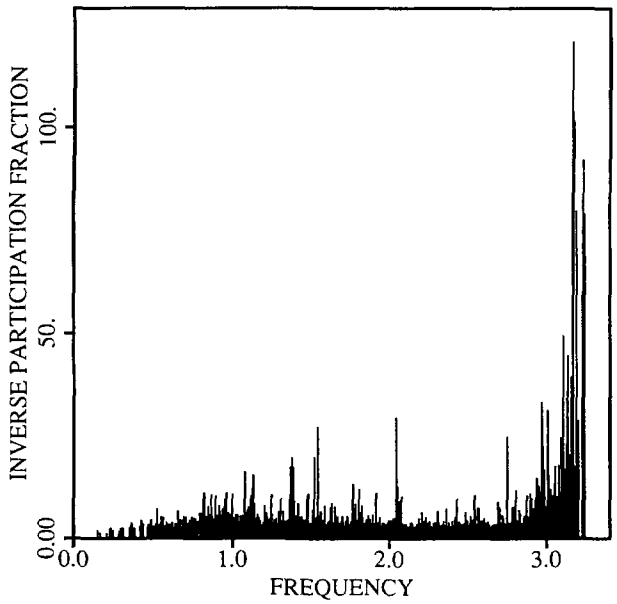

a)

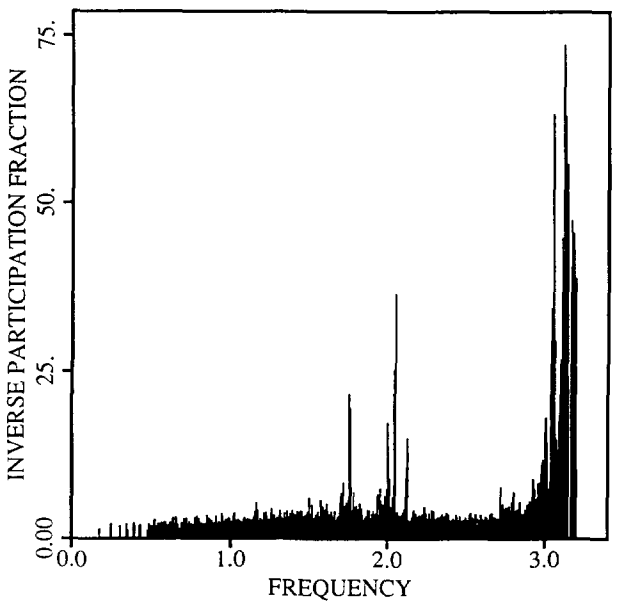

b)

Fig.10. — The inverse participation fraction for a cluster with free boundary conditions (10a), the symmetrized 5/3-approximant (10b) and a randomized configuration of the 932-approximant(10c). The figures 10b and 10c contain only the contributions from k-vectors yielding real dynamical matrices.

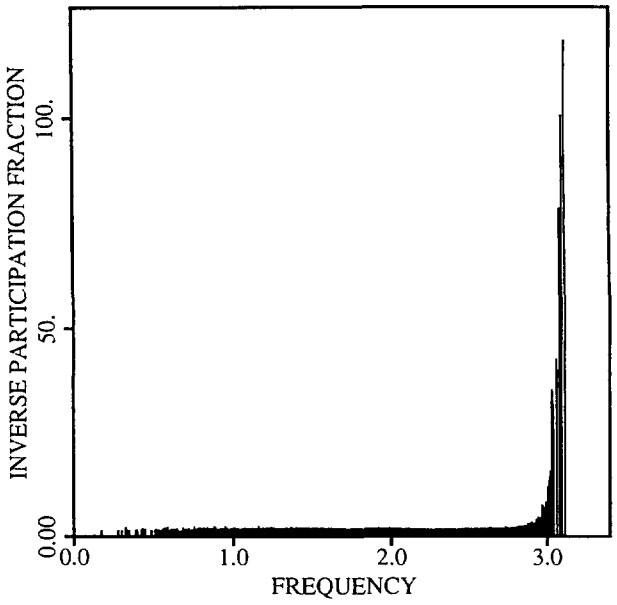

c)

Fig.10. — (continued)

we considered (those yielding real dynamical matrices) this is a good choice, since the standing wave solutions for these k-vectors can be normalized over the atoms inside this unit cell. With the formulae (21) and (22), taking s equal to 1, one can easily produce the results for systems containing K unit cells. In the limit of K tending to infinity one finds the expected result for periodic structures. By considering larger and larger approximants of the i-PT one can observe whether the lower bound of the support of the $S(\alpha)$-function does or does not approach to the value 1 at $\alpha = 1$. In the latter case the scaling behaviour is not normally extended.

To learn more about the character of the states with high IPF we have calculated for the symmetrized 2/1-, 3/2-, 5/3- and 8/5-approximants the $S(\alpha)$-function for the state with the highest IPF which transforms according to the standard representation. The result, which is shown in figure 11, suggests that these states scale as critical states, since the support of the $S(\alpha)$-function does not decrease for the higher approximants. In the quasiperiodic limit one can thus expect critical states at high frequency.

A number of the highest eigenvalues and corresponding eigenvectors for an irreducible matrix block belonging to the symmetrized 8/5-approximant, which has 10563 atoms in the unit cell, was computed using a Lanczos algorithm without reorthogonalization. In this algorithm the matrix is not changed and only matrix-vector multiplications are needed. Therefore it makes efficient use of the sparseness of the matrix. The algorithm, which serves to find (part of or all) the eigenvalues and, if needed, the eigenvectors of large and sparse hermitian matrices, is described in reference [12].

Figure 12 shows the $S(\alpha)$-function for the states with the highest IPF for the perfect and two randomized tetragonal 932-approximants. The support for both randomized approximants is somewhat wider, which means that for these high frequency states criticality is enhanced by randomization. Moreover the two curves for the randomized cases are very similar, so that one may expect that they are typical for randomized configurations.

From figure 10 it becomes clear that only a minority of the states has high IPF. The other

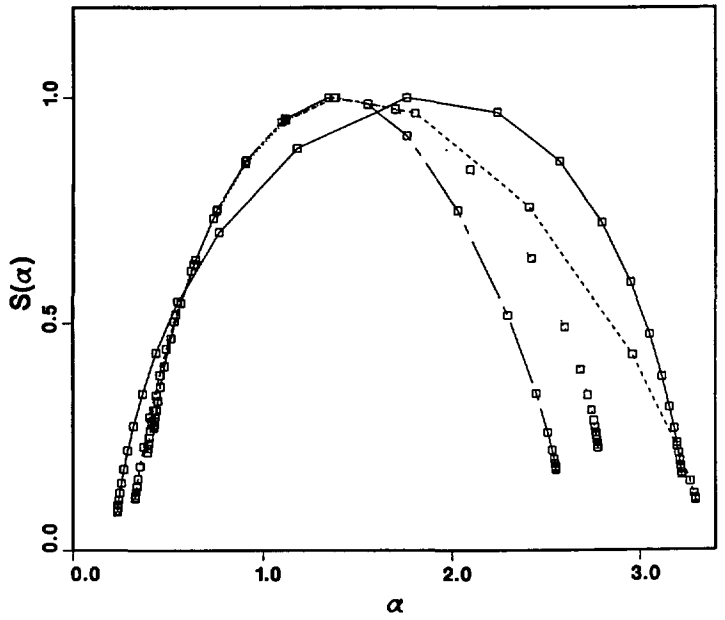

Fig.11. — The entropy functions for the state with the highest inverse participation ratio at $\mathbf{k} = 0$ in the symmetrized 2/1-,3/2-, 5/3- and 8/5-approximants, transforming according to the defining representation (dotted, dashed, chaindashed and solid curves, respectively).

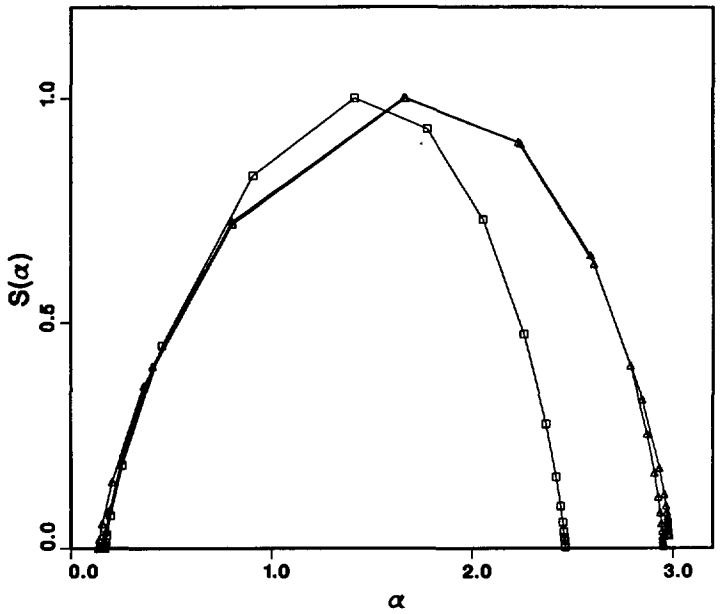

Fig.12. — The entropy functions for the state with highest inverse participation ratio at $\mathbf{k} = 0$ in the 932-approximant (square marks) and two of its randomizations (triangular marks).

states have a much lower IPF, and may also have a different scaling behaviour. To study this we propose the following analysis.

In the thermodynamical formalism of the multifractal analysis there is a one to one relation between β and α (recall that they are conjugate variables of a Legendre transformation). For $\beta > 0$ the 'partition function' is dominated by the large p_i (i.e. larger than $1/L$), which corresponds to α-values smaller than 1. For $\beta < 0$ the small p_i dominate, which corresponds to α bigger than 1. Due to the normalization constraint for the p_i's, the support of the $S(\alpha)$-function must contain the value $\alpha = 1$. Contributions with $\alpha > 1$ must be compensated by contributions with $\alpha < 1$, and vice versa. In this sense the part of the $S(\alpha)$-function with $\alpha < 1$ contains also information on the part with $\alpha > 1$. Therefore we propose the following definition of moment:

$$\mu = \frac{\sum_{k=1}^{k_{max}} \alpha_k S(\alpha_k)}{\sum_{k=1}^{k_{max}} S(\alpha_k)} \tag{30}$$

where α_k corresponds to integer β-values $\beta = k$. Because the summation runs over positive integer β-values the corresponding α-values lie on the left shoulder of the $S(\alpha)$-function. Numerically we found this quantity μ the most effective way to characterize the $S(\alpha)$-function (see also the discussion of the mono-atomic chain above). For the maximal β-value in the summation we chose $k_{max} = 7$, which seems a reasonable choice. In terms of μ, completely extended states correspond to $\mu = 1$, and localized states to $\mu = 0$.

The moment μ is defined for each eigenstate. Figure 13a shows the normalized density of states as a function of μ for the symmetrized 2/1-, 3/2- and 5/3-approximants. Again only the states belonging to wave vectors with high symmetry were considered. One observes that the DOS is strongly peaked around some value of μ in all three cases, and that only a few states, those with high IPF, have a relatively low μ-value. One also observes that the peak is shifted to the right, towards $\mu = 1$, for the higher approximants.

A better view of the scaling behaviour is given by figure 13b which shows the DOS for the same three rational approximants, but now for systems of equal 'size'. This was done by making use of formulae (21) and (22) with $s = 1$, allowing non-integer values of K such that the 'size' of the system was equal to the 'size' of the 5/3-approximant in all three cases. This figure shows that the curves for the 3/2- and 5/3-approximants are very close, which suggests that the majority of the states scale as normal extended states, i.e. in the limit the position of the peak will approach closely the value $\mu = 1$.

The result for the 2/1-approximant does not completely support this conclusion, but since we are interested only in the incommensurate limit we may argue that the 2/1-approximant is just too far away from that limit. We admit however that it might be too early to draw definitive conclusions from the behaviour of only two successive approximants.

The results for the i-PT are again compared with the results for the Fibonacci chain. Figure 14 shows the IPF together with the integrated density of states as a function of frequency for the 610-approximant of the Fibonacci chain. Qualitatively the only difference with the 3-dimensional case is that states start to have higher IPF already at much lower frequency for the Fibonacci chain.

Figure 15a shows the normalized DOS as a function of μ for the same three rational approximants of the Fibonacci chain as in the previous section. In each case the wave numbers $k = m\pi/Ma$ ($m = 0, 1.., M$) were considered, where a is the primitive lattice constant. The standing wave solutions were normalized over a unit cell containing M primitive unit cells.

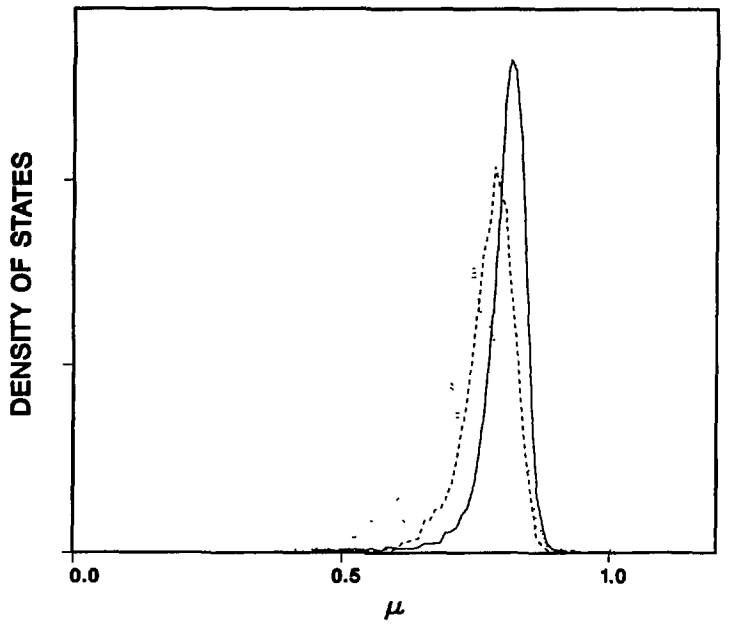

a)

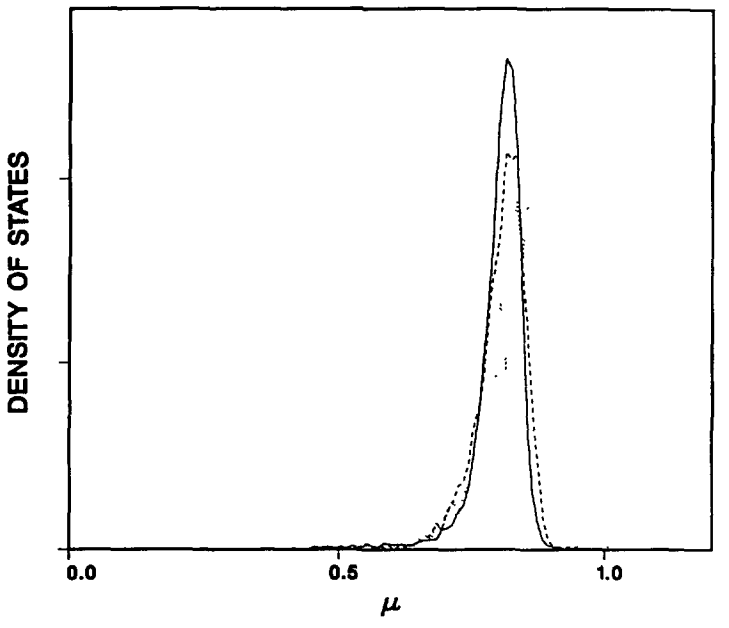

b)

Fig.13. — a) The density of states as a function of μ for the symmetrized 2/1-, 3/2- and 5/3-approximants (dotted, dashed and solid lines, respectively). b) Same as figure 13a, but for systems of equal 'size'.

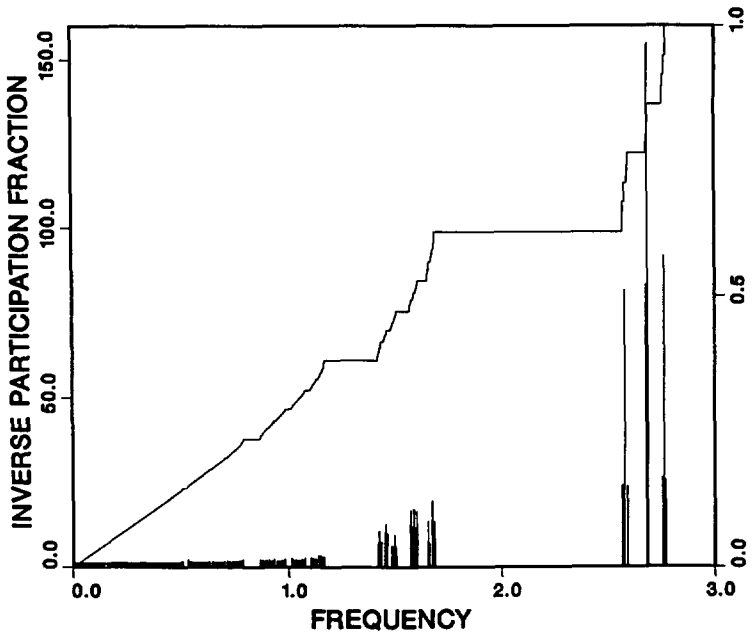

Fig.14. — The inverse participation fraction (IPF) and the normalized integrated density of states (IDOS) for an approximant of the Fibonacci chain having 610 atoms in the primitive unit cell. Labels on the left and the right vertical axis are for the IPF and the IDOS, respectively. The spring constants were taken equal to 1 and 3 for respectively the long and the short interval.

For the 34-, 144- and 610-approximants the value of M was taken equal to respectively 48, 12 and 3, so that the number of states considered were respectively 1666, 1872 and 2440. For the two smaller approximants the S-function was 'renormalized' to the 'size' $L = 3 \times 610 = 1830$, which is the 'size' that correspond to the 610-approximant.

Finally figure 15b shows the relative contributions from the k-values yielding a real dynamical matrix and other k-values to the density of states as a function of μ. This picture shows that these contributions, apart from a weight factor, are qualitatively the same, so that, at least for the Fibonacci chain, it is justified to consider only a certain subset of wave numbers. Therefore we expect that this is also true for the i-PT, so that the result of figure 13 is qualitatively equal to the result one would obtain by including all states.

Comparing the results of figures 13 and 15 one must conclude that the phonon states in the Fibonacci chain behave much more critically then in the i-PT. This may be not quite in agreement with what we expect from the scaling behaviour of the spectra. Obviously the relation between the scaling behaviour of the spectrum and the character of the eigenstates depends on the dimension, at least for structures which are not lattice periodic. We remark that also for 1-dimensional aperiodic systems the relation between the scaling behaviour of the spectrum and the character of the eigenstates is not always so strictly determined. This was already shown by Axel and Peyriere [13] for the Thue-Morse chain, which has a singularly continuous spectrum together with extended states. For 3-dimensional systems the relation may be even less evident. It is, for example, not clear what band overlaps, which occur only for 2- and 3-dimensional systems, mean for the character of the eigenstates. In a certain sense band overlaps in $(\omega, \mathbf{k})$-space correspond to more degrees of freedom for the atoms in real space, and

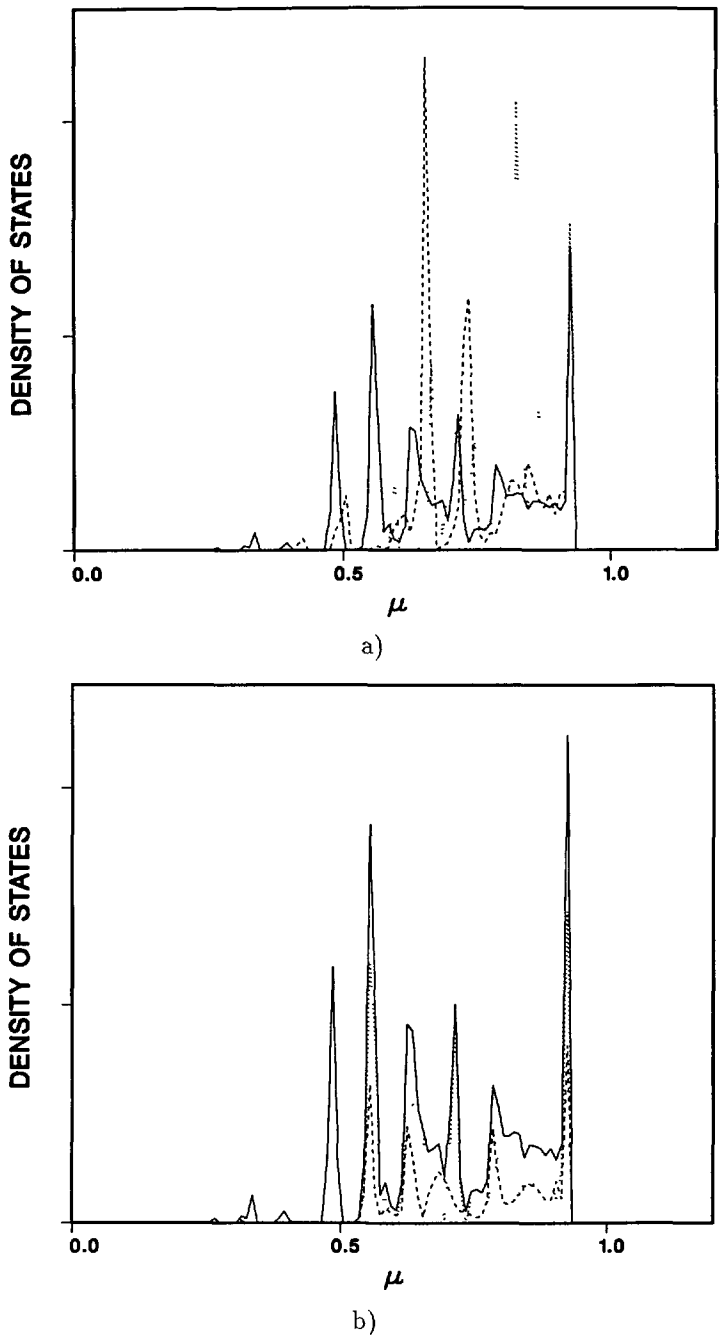

Fig.15. — a) The density of states as a function of μ for three rational approximants of the Fibonacci chain having 34, 144 and 610 atoms in the primitive unit cells (dotted, dashed and solid lines, respectively). The eigenstates were first normalized over respectively 1632, 1728 and 1830 atoms, and then for the first two systems the S-function was 'renormalized' to the 'size' $L = 1830$. b) The respective contributions from the $k = 0$ and $k = \pi/a$ modes (dashed line) and the modes corresponding to two other k-values (dotted line) to the total density of states (solid line) as a function of μ.

intuitively one may expect that this will help to avoid localized states. Certainly, a lot more research will have to be done in order to fully understand the relation between the spectrum and the character of the eigenstates, especially for systems in more than one dimension.

6. Conclusions.

Having studied the lattice dynamics of several models for the icosahedral quasicrystals the following (preliminary) conclusions can be drawn.

Globally the vibrational density of states as a function of frequency is rather structureless, i.e. it does not contain strong peaks. It is even more smoothed by randomization. Only on a smaller scale one may find more structure.

The scaling behaviour for the bandspectrum is different from the scaling behaviour for an absolutely continuous spectrum and it is likely that the spectrum for the quasiperiodic limit has to be classified as singularly continuous. This also holds true for the randomized tilings.

Concerning the character of the eigenstates we found very similar results for all models we have considered, namely that most states have an extended character, and that only relatively few states at the very upper end of the spectrum have a more localized character. A multifractal analysis of these latter states shows that their scaling behaviour is critical, so that in the quasiperiodic limit one can expect critical states at high frequency. For all other states the multifractal analysis showed a scaling behaviour that corresponds to extended states.

Acknowledgments.

This work has been supported by the 'Stichting voor Fundamenteel Onderzoek der Materie' (F.O.M.) with financial support of the 'Nederlandse Organisatie voor Wetenschappelijk Onderzoek' (N.W.O.). The randomization program we used is partially based on a code written by L.H. Tang. We thank him for freely sharing his code with us.

References

[1] Los J. and Janssen T., *J. Phys. Cond. Matt.* **2** (1990) 9553.

[2] Shechtman D., Blech I., Gratias D. and Cahn J.W., *Phys. Rev. Lett.* **53** (1984) 1951-1953.

[3] Henley C.L., Random Tiling Models, in Quasicrystals: The State of the Art, P.J. Steinhardt and D.P. DiVincenzo Eds. (World Scientific, 1991).

[4] Tang L.H., *Phys. Rev. Lett.* **64** (1990) 2390.

[5] Luck J.M. and Petritis D., *J. Stat. Phys.* **42** (1986) 289.

[6] Kohmoto M., Banavar J.R., *Phys. Rev. B* **34** (1986) 563.

[7] Kohmoto M., *Phys. Rev. A* **37** (1988) 1345.

[8] Katz A. and Duneau M., *J. Phys. France* **47** (1986) 181.

[9] Suck J.B., *Phys. Rev. Lett.* **59** (1987) 102.

[10] Janssen T., *Europhys. Lett.* **14** (1991) 131.

[11] Janssen T. and Kohmoto M., *Phys. Rev. B* **38** (1988) 5811.

[12] Cullum J.K. and Willoughby R.A., Lanczos algorithms for large symmetric eigenvalue computation (Birkhäuser, 1985).

[13] Axel F. and Peyriere J., *J. Stat. Phys.* **57** (1989) 1013.